gamma-ray transition is that the 2.21-Mev state and either the 2.98- or 3.00-Mev state are the $\frac{7}{2}^+$ and $9/2^+$ members of the $K=\frac{5}{2}$ rotational band as indicated in Fig. 5. The 3.0-Mev state would then be expected to decay strongly to the 2.21-Mev state by an $M1$ transition and more weakly to other states because of higher spin differences.

ACKNOWLEDGMENTS

The authors are indebted to Professor M. B. Sampson for his advice and assistance in achieving optimum cyclotron performance which greatly facilitated these experiments. They would also like to acknowledge the encouragement and support of Professor A. C. G. Mitchell which made this work possible.

PHYSICAL REVIEW VOLUME 122, NUMBER 5 JUNE 1, 1961

Coupled Square Well Model for Elastic Scattering*

D. E. BILHORN, *Rice University, Houston, Texas*

AND

W. TOBOCMAN,† *Case Institute of Technology, Cleveland, Ohio*

(Received January 30, 1961).

A simple model for s-wave neutron scattering is provided by representing the scattering potential by a pair of coupled square wells. Such a model produces resonances that exhibit the giant resonance effect. We have compared isolated resonances given by this model for two types of coupling with the Breit-Wigner formula. We find that for a resonance with a width of about 16 kev, the resonant part of the scattering does indeed have the Breit-Wigner form. The resonance energy is found to be considerably shifted from the energy of the bound state that exists in the zero-coupling-strength limit. Also the nonresonant part of the scattering amplitude is considerably different from both the hard-sphere scattering amplitude and the zero-coupling-strength limit scattering amplitude. This last result is in accord with expectations based on R-matrix theory.

IN a recent paper,[1] a simple model (denoted hereafter by A) for the elastic scattering of s-wave neutrons was discussed. Sharp resonances were introduced into the slowly varying optical-model scattering amplitude by weakly coupling a second mode of motion (the compound-nucleus mode) to the motion in the incident channel. It was shown that the reduced widths of the sharp resonances in the model exhibit the giant-resonance behavior which has been observed in nuclear scattering. Here we shall consider the application of the Breit-Wigner single-level formula to these sharp resonances. The results will be compared with those for another type of simple model (B) for the same process.

The scattering interaction for model A consists of a square-well potential modified by allowing transmission through the origin through a square barrier to another well. The second square well provides the second (compound nucleus) mode of motion. Explicitly, the potential has the form

$$\begin{aligned} V(r)&=0, && r>R_1\\ &=-V_1, && 0<r<R_1\\ &=V_2, && -R_2<r<0\\ &=-V_3, && -(R_2+R_3)<r<-R_2\\ &=\infty, && r<-(R_2+R_3). \end{aligned} \tag{1}$$

For $r>R_1$ the radial wave function has the form $r\psi=e^{-ikr}-\eta e^{ikr}$. The amplitude of the outgoing wave, η, can be written in terms of the hard sphere amplitude $\eta_{\text{H.S.}}$ as

$$\eta=-\eta_{\text{H.S.}}S,$$

where

$$\begin{aligned} &\eta_{\text{H.S.}}=e^{2i\xi}, \quad \xi=-kR_1,\\ &S=e^{2i\Phi}, \quad \Phi=-\arctan(Z/\Gamma_1),\\ &Z=\frac{\cot K_1R_1-b}{1+b\cot K_1R_1}=\cot(K_1R_1+y), \qquad (2)\\ &b=\tan y=b_0/\Gamma_2,\\ &b_0=\frac{\tanh K_2R_2+\Gamma_3\tan K_3R_3}{1+\Gamma_3\tan K_3R_3\tanh K_2R_2}, \end{aligned}$$

K_1, K_2, K_3 are the wave numbers for the particle in potentials V_1, V_2, V_3 and $\Gamma_1=k/K_1$, $\Gamma_2=K_2/K_1$, $\Gamma_3=K_2/K_3$.

The scattering amplitude is proportional to $A=1-\eta=1+\eta_{\text{H.S.}}S$. In the limit of zero coupling ($V_2=\infty$) we have $\Gamma_2=\infty$, so b becomes zero and $Z=\cot K_1R_1$ which gives the slowly varying amplitude A_0 due to the square well V_1. For weak coupling ($K_2\gg k, K_1, K_3$), Γ_2 is large and it becomes possible to write b_0 in the form:

$$\begin{aligned} &b_0=1-\delta\beta,\\ &\delta=2e^{-2K_2R_2}\ll 1, \qquad (3)\\ &\beta=(1-\Gamma_3\tan K_3R_3)/[1+(1-\delta)\Gamma_3\tan K_3R_3]. \end{aligned}$$

* Supported in part by the National Science Foundation.

† On leave of absence from Rice University, Houston, Texas.

[1] W. Tobocman and D. E. Bilhorn, Phys. Rev. **115**, 1275 (1959).

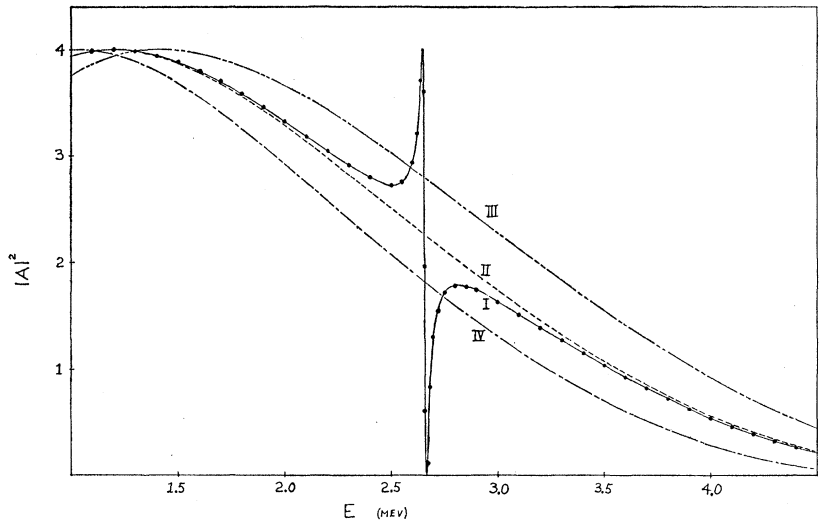

FIG. 1. Cross section for s-wave neutron elastic scattering according to model A. Parameters are $R_1=R_3=6$ fermi, $R_2=0.48$ fermi, $V_1=40$ Mev, $V_2=500$ Mev, $V_3=45$ Mev. Curve I is the exact cross section $|A|^2$ given by the model, curve II the background cross section $|\bar{A}|^2$, curve III the cross section $|A_{\text{H.S.}}|^2$ for scattering from a hard sphere of radius R_1, curve IV the cross section $|A_0|^2$ for scattering from the uncoupled optical well V_1, and the dots are the Breit-Wigner fit $|\bar{A}+A_{\text{B.W.}}|^2$ to the exact cross section $|A|^2$. The parameters used in the Breit-Wigner formula are $E_0=2.655$ Mev and $\Gamma_0=18$ kev.

Thus b_0 is close to 1 except when $1+(1-\delta)\Gamma_3\tan K_3R_3$ is near zero, where b_0 varies rapidly, giving rise to a resonance. Thus the scattering amplitude far from a resonance takes the form

$$\begin{aligned}&\bar{A}\cong 1+\eta_{\text{H.S.}}\bar{S},\\&\bar{S}=\exp(2i\bar{\Phi}),\quad \bar{\Phi}=-\arctan(\bar{Z}/\Gamma_1),\\&\bar{Z}=\cot[K_1R_1+\arctan(1/\Gamma_2)],\end{aligned}\tag{4}$$

and we may write the exact amplitude as $A=\bar{A}+A_R$, where $A_R=\eta_{\text{H.S.}}(S-\bar{S})$ is to be identified as the contribution to the scattering amplitude due to the resonance. Since A_R may be written $A_R=\eta_{\text{H.S.}}(-\bar{S})(1+S_R)$, and $1+S_R=(-\bar{S})^{-1}S=\exp[2i(\Phi-\bar{\Phi}-\frac{1}{2}\pi)]$, it is $(1+S_R)$ that is to be compared with the Breit-Wigner single-level dispersion form $i\Gamma/(E-E_0+\frac{1}{2}i\Gamma)$ or $\Phi-\bar{\Phi}-\frac{1}{2}\pi$ is to be compared with $\arctan[(E-E_0)/\frac{1}{2}\Gamma]$. The factor $\eta_{\text{H.S.}}\times(-\bar{S})$ gives the relative phase of $\bar{A}$ and $(1+S_R)$.

Numerical calculations show that $(1+S_R)$ does indeed have the Breit-Wigner form, allowing us to identify $\bar{A}$ as the "potential" scattering amplitude. This amplitude is neither a hard-sphere amplitude, nor simply the amplitude $A_0=1+\eta_{\text{H.S.}}\exp(-2i\Gamma_1^{-1}\cot K_1R_2)$ due to the uncoupled well V_1. In the weak coupling approximation, $\bar{A}$ has essentially the same form as A_0 except that the effective radius in the factor $\bar{Z}$ has become increased $[\bar{Z}\simeq\cot(K_1R+\Gamma_2^{-1})=\cot K_1(R_1+K_2^{-1})]$. If we think in terms of the R-matrix formalism,[2] this is the manifestation of the effect of distant resonances on the background amplitude for this model. Hence, if the background amplitude $\bar{A}$ is to be represented either by a hard-sphere amplitude or a square-well amplitude, some parameter must be energy dependent, for example, the radius of the hard sphere or the depth of the square well. In Fig. 1, the cross section $|A|^2$ of a typical isolated resonance of the model is presented, together with the cross sections: $|A_{\text{H.S.}}|^2$ for hard-sphere scattering from a sphere of radius R_1, $|A_0|^2$ for scattering from the uncoupled well V_1, the background cross section $|\bar{A}|^2$, and the Breit-Wigner fit $|\bar{A}+A_{\text{B.W.}}|^2$ where $A_{\text{B.W.}}=\eta_{\text{H.S.}}(-\bar{S})i\Gamma_0/(E-E_0+\frac{1}{2}i\Gamma_0)$. In Fig. 2, curve I shows the energy dependence of the hard-sphere radius $R(E)$ needed to reproduce the background amplitude $\bar{A}$. The parameters for this case are $R_1=R_3=6$ fermi, $R_2=0.48$ f, $V_1=40$ Mev, $V_2=500$ Mev, $V_3=45$ Mev, and the Breit-Wigner parameters are $E_0=2.655$ Mev, $\Gamma_0=18$ kev.

Another model (B), which couples a second mode of motion to that of the incident particle but which employs a different method of coupling from that discussed above, is provided by coupling two Schrödinger equations by means of a square potential.[3,4] Explicitly we write

$$\begin{aligned}&(E-H_1)\psi_1=V_{12}\psi_2,\quad (E-H_2)\psi_2=V_{21}\psi_1,\\&H_1=T+V_1,\quad H_2=T+V_2,\quad T=-\frac{\hbar^2}{2m}\frac{d^2}{dr^2},\end{aligned}\tag{5}$$

$$\begin{aligned}V_1(r)&=0, && r>R_1\\&=-V_1, && 0<r<R_1\\V_2(r)&=\infty, && r\geq R_2\\&=-V_2, && 0<r<R_2\\V_{12}(r)&=V_{21}^*(r)=0, && r>R\\&=V_{12}+iW_{12}, && 0<r<R\end{aligned}\tag{6}$$

and subject to $R\leq R_1, R_2$. If we take $R=R_1(\leq R_2)$ then

[2] A. M. Lane and R. G. Thomas, Revs. Modern Phys. **30**, 273 (1958).

[3] We are grateful to Dr. L. C. Biedenharn and Dr. M. H. Kalos who both independently suggested this model to us.

[4] T. A. Tombrello and G. C. Phillips, Nuclear Phys. (to be published).

the coupling of the optical mode to the compound nucleus mode takes place over the entire range of the optical potential, in contrast to model A, in which the coupling was concentrated at the origin of the optical potential. Thus, the method of coupling in the two models is of quite different character, and we may then gain information as to which properties of a system of two coupled square wells are sensitive to the details of the coupling.

For $r>R_1$, ψ_1 has the form $\psi_1=e^{-ikr}-\eta e^{ikr}$ and ψ_2 is zero for $r\geq R_2$. The scattering amplitude is then proportional to $A=1-\eta$ and η may be calculated once the coupled equations have been solved. This is readily done since the potentials involved are constants in the range of r for which the equations are coupled. One finds that for the case $R=R_1\leq R_2$, η has the form:

$$\eta=-\eta_{\text{H.S.}}s,$$

$$s=e^{2i\varphi},\quad \varphi=-\arctan(z/\gamma_1),\tag{7}$$

$$z=\frac{\kappa_1\cot\kappa_1R_1+\alpha\kappa_2\cot\kappa_2R_1}{\kappa_1(1+\alpha)},$$

$$\alpha=\epsilon^2\frac{\kappa_1\cot\kappa_1R_1+K_2\cot K_2(R_2-R_1)}{\kappa_2\cot\kappa_2R_1+K_2\cot K_2(R_2-R_1)},$$

$$\epsilon^2=\frac{2m}{\hbar^2}\frac{V_{12}^2+W_{12}^2}{(K_2^2-\kappa_1^2)^2},$$

$$\gamma_1=k/\kappa_1,\tag{8}$$

$$\kappa_1^2=\tfrac{1}{2}\{K_1^2+K_2^2+[(K_1^2-K_2^2)^2+4(V_{12}^2+W_{12}^2)2m/\hbar^2]^{\frac{1}{2}}\},$$

$$\kappa_2^2=\tfrac{1}{2}\{K_1^2+K_2^2-[(K_1^2-K_2^2)^2+4(V_{12}^2+W_{12}^2)2m/\hbar^2]^{\frac{1}{2}}\},$$

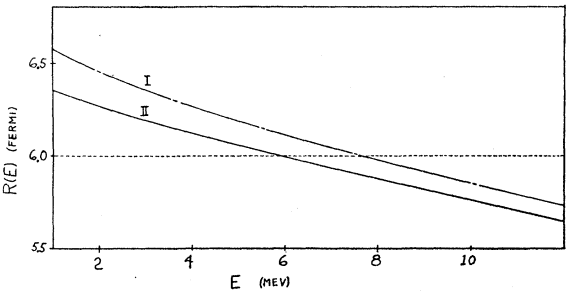

FIG. 2. Energy dependence of hard sphere radius $R(E)$ needed to fit background cross section $|\bar{A}|^2$ with the cross section due to hard-sphere scattering. Curve I is the $R(E)$ needed for the cross section obtained in model A (Fig. 1) while curve II is the $R(E)$ needed for cross section due to model B (shown in Fig. 3).

where K_1, K_2 are the wave numbers in the uncoupled wells V_1, V_2, respectively.

The expression, z, is not as easy to analyze as was Z. We have not been able to find a simple expression for z when the energy is far from an isolated resonance. However, one can numerically and graphically determine a background amplitude $\bar{A}=(1+\eta_{\text{H.S.}}\bar{s})$ such that it, plus a Breit-Wigner amplitude [again with the relative phase given by $\eta_{\text{H.S.}}(-\bar{s})$] gives a good approximation to the exact amplitude A.

The scattering cross section for a typical isolated resonance for this model is shown in Fig. 3 where again $|A_{\text{H.S.}}|^2$ is the hard-sphere cross section for a sphere of radius R_1, $|A_0|^2$ the cross section for the uncoupled well V_1, $|\bar{A}|^2$ the background cross section, $|A|^2$ the exact cross section, and $|\bar{A}+A_{\text{B.W.}}|^2$ the Breit-Wigner fit. Curve II in Fig. 2 shows the energy dependence of the hard-sphere radius $R(E)$ needed to fit the background amplitude $\bar{A}$. The parameters for this case are $R_1=6$ fermi, $R_2=2R_1=12$ fermi, $V_1=40$ Mev, $V_2=45$ Mev, $V_{12}=0.16$ Mev, $W_{12}=0$; and the Breit-Wigner

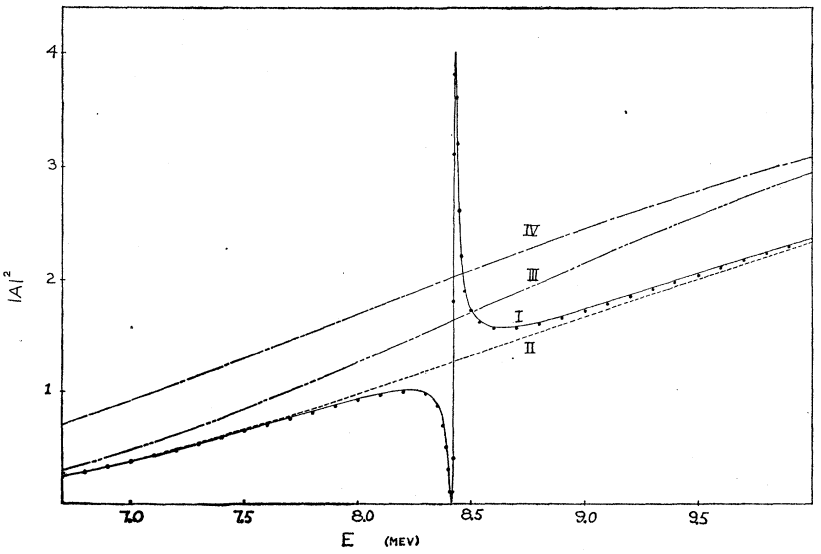

FIG. 3. Cross section for s-wave neutron scattering according to model B. Parameters are $R_1=6$ fermis, $R_2=2R_1=12$ fermis, $V_1=40$ Mev, $V_2=45$ Mev, $V_{12}=0.16$ Mev, $W_{12}=0$. Curve I is the exact cross section $|A|^2$ given by the model, curve II the background cross section $|\bar{A}|^2$, curve III the cross section $|A_{\text{H.S.}}|^2$ for scattering from a hard sphere of radius R_1, curve IV the cross section $|A_0|^2$ for scattering from the uncoupled optical well V_1, and the dots are the Breit-Wigner fit $|\bar{A}+A_{\text{B.W.}}|^2$ to the exact cross section $|A|^2$. The parameters used in the Breit-Wigner formula are $E_0=8.427$ Mev and $\Gamma_0=15$ kev.

parameters are $E_0=8.427$ Mev, $\Gamma_0=15$ kev. Again, we see that the background cross section is significantly different from the hard sphere or optical potential cross sections. Also the energy dependent hard sphere radius needed to fit the background cross section shows qualitatively the same behavior as in model A.

The parameters have been chosen in both cases, so that the energy of the resonance when the coupling goes to zero, $\bar{E}$, is the same. This energy is that of the nearest level in the uncoupled infinite square well representing the compound nucleus mode of motion. For these parameters, this energy is 5.904 Mev. (The compound nucleus well in model B has twice the radius as the compound nucleus well in model A so that the level density is twice as great, but the levels in such a well are separated by energies of the order of 20 Mev at this energy. Therefore, the separation of resonances in the scattering cross section is large compared to the widths of the resonances when the coupling is weak. Thus we are dealing with well isolated resonances in both cases.) The strength of the coupling in both models has been adjusted so that the total widths of the resonances, Γ_0, is small, and so that Γ_0 is approximately the same for the two resonances. In this case, the reduced widths $\gamma^2=\Gamma/2kR_1$ in both models will be roughly the same if the resonance energies are the same. This means that the probability of forming the compound mode of motion in both cases is essentially the same. Using this effect as a measure of the coupling, we can then say the strengths of the coupling in the two cases are roughly the same.

There are two points that can be made. One is that in general the shape of the resonance is not strongly model dependent, while the level shift and the background cross section are quite sensitive to the details of the coupling mechanism. The second point arises from the realization that the widths of the resonances shown in Figs. 1 and 3 are small in comparison with experimentally observed widths. The reduced widths are 4 and 2 kev for models A and B, respectively. Thus the coupling is weak. However, the shifts in the resonance energies from $\bar{E}$, the Δ's, are large ($\Delta\cong-3.3$ Mev in model A, $\Delta\simeq+2.5$ Mev in model B). Also, even though the resonances are well isolated for these cases and the coupling is weak, the background cross section differs significantly from the zero-coupling cross section. Therefore it is evident that even in the weak-coupling limit, sizable effects can occur.

PHYSICAL REVIEW VOLUME 122, NUMBER 5 JUNE 1, 1961

Fluorescent Response of Scintillation Crystals to Heavy Ions*

E. NEWMAN, A. M. SMITH, AND F. E. STEIGERT
Yale University, New Haven, Connecticut
(Received January 27, 1961)

The light output of CsI(Tl) was measured as a function of energy for incident ions of B^{10}, B^{11}, C^{12}, N^{14}, O^{16}, and F^{19}. The response of NE 102 plastic and anthracene scintillators was also measured for ions of N^{14} and O^{16}, respectively. The response of CsI was essentially linear for energies above 6 Mev/A, where A is the mass number of the incident ion. The NE 102 was linear for energies above 4 Mev/A. The anthracene data showed slight curvature even at 9 Mev/A. It would appear that the response of CsI differs somewhat among crystal samples.

INTRODUCTION

DURING the search for suitable particle detectors for heavy ions, a systematic survey of various scintillation crystals was undertaken by various groups at this laboratory. As has already been reported,[1,2] the alkali halides proved generally superior in performance because of their higher light output and correspondingly better resolution. The CsI(Tl) crystals demonstrated one rather strange characteristic, however. There appeared to be a reproducible difference in luminescence among crystals obtained at different times from different sources. This variation could be reliably associated with the pulse height ratio between the ThC and ThC' alpha particle groups. The organic and plastic scintillators used, as well as having a total light output somewhat lower than that of the CsI, showed rather significant differences in general behavior. Hopefully, in these variations lies the clue to a better understanding of the mechanisms involved in the scintillation process.

EXPERIMENTAL RESULTS

The experimental data were obtained in the manner previously described.[1] Particle beams from the Yale heavy-ion linear accelerator were magnetically analyzed, degraded with nickel absorbing foils, and then reanalyzed in a magnet spectrometer. The detection system consisted of $\frac{1}{2}$-in. diameter by $\frac{1}{2}$- to 1-mm thick crystals

* Supported in part by the Office of Naval Research and the Atomic Energy Commission.
[1] E. Newman and F. E. Steigert, Phys. Rev. **118**, 1575 (1960); see also, Bull. Am. Phys. Soc. 4, 51 (1959); 4, 270 (1959).
[2] A. R. Quinton, C. E. Anderson, and W. J. Knox, Phys. Rev. **115**, 886 (1959).